The Journal of Neuroscience, May 1, 1998, *18*(9):3327–3335

Development of the Mouse Inner Ear and Origin of Its Sensory Organs

Hakim Morsli,[1] Daniel Choo,[1] Allen Ryan,[2] Randy Johnson,[3] and Doris K. Wu[1]

[1]National Institute on Deafness and Other Communication Disorders, Rockville, Maryland 20850, [2]Departments of Surgery/Otolaryngology and Neurosciences, School of Medicine, and Veterans Administration Medical Center, University of California at San Diego, La Jolla, California 92093-0666, and [3]M. D. Anderson Cancer Center, University of Texas, Department of Biochemistry and Molecular Biology, Houston, Texas 77030-4095

The molecular mechanisms dictating the morphogenesis and differentiation of the mammalian inner ear are largely unknown. To better elucidate the normal development of this organ, two approaches were taken. First, the membranous labyrinths of mouse inner ears ranging from 10.25 to 17 d postcoitum (dpc) were filled with paint to reveal their gross development. Particular attention was focused on the developing utricle, saccule, and cochlea. Second, we used bone morphogenetic protein 4 (*BMP4*) and lunatic fringe (*Fng*) as molecular markers to identify the origin of the sensory structures. Our data showed that *BMP4* was an early marker for the superior, lateral, and posterior cristae, whereas *Fng* served as an early marker for the macula utriculi, macula sacculi, and the sensory portion of the cochlea. The posterior crista was the first organ to appear at 11.5 dpc and was followed by the superior crista, the lateral crista, and the macula utriculi at 12 dpc. The macula sacculi and the cochlea were present at 12 dpc but became distinguishable from each other by 13 dpc. Based on the gene expression patterns, the anterior and lateral cristae may share a common origin. Similarly, three sensory organs, the macula utriculi, macula sacculi, and cochlea, seem to arise from a single region of the otocyst.

Key words: inner ear development; sensory organs; lunatic fringe; BMP4*;* NT-3*;* Brn3.1

The mammalian inner ear is an unusually complex organ. The vestibular sensory organs including the macula utriculi, macula sacculi, and cristae are responsible for detecting gravity and linear and angular acceleration. These functions are necessary for maintaining normal balance. The coiled cochlea contains the auditory machinery necessary for hearing. One of the most remarkable aspects of the inner ear is that its elaborate three-dimensional structure, as well as the ganglion that innervates its sensory organs, arise from a simple hollow sphere of epithelium, the otic vesicle. To better visualize the normal morphogenesis of the mouse inner ear, and in particular, the cochlea, a solution of white latex paint was injected into the lumen of mouse inner ears at different stages of development (Martin and Swanson, 1993). The gross anatomical changes of the inner ear were correlated with the appearance of each sensory organ that was identified by genes specifically expressed in sensory regions before histological differentiation. One such candidate gene was bone morphogenetic protein 4 (*BMP4*), a member of the transforming growth factor-β gene family. Previous studies showed that *BMP4* is an early marker for all the presumptive sensory organs in the chicken inner ear (Wu and Oh, 1996). The early *BMP4* gene expression pattern in the chicken otocyst (an anterior and posterior focus) appears to be similar to those observed in *Xenopus* (Hemmati-Brivanlou and Thomsen, 1995) and mouse (Jones et al., 1991) otocysts. However, although *BMP4* is expressed in hair cells of the chicken basilar papilla (cochlea) before hatching (Oh et al., 1996), it has been reported to be expressed exclusively by Claudius' cells of the mouse cochlea (Takemura et al., 1996).

Lunatic fringe (*Fng*), the murine homolog of *Drosophila* fringe, has been implicated in the formation of boundaries during embryogenesis (Cohen et al., 1997; Johnston et al., 1997). In the otic vesicle, *Fng* is expressed in restricted domains in both the mouse and the chicken (Johnston et al., 1997; Laufer et al., 1997). More detailed studies of the chicken inner ear indicate that *Fng* is expressed in some presumptive sensory organs at early stages (F. Nunes and D. K. Wu, unpublished observations).

Neurotrophin-3 (*NT-3*) and Brain-3.1 (*Brn-3.1*) were also considered good candidates for sensory organ markers. *NT-3* has been reported to be expressed in hair cells of the embryonic rat cochlea (Ylikoski et al., 1993; Wheeler et al., 1994). A more recent study suggests that *NT-3* expression in the mouse may be broader and concentrated in supporting cells of the inner ear (Fritzsch et al., 1997a,b). *Brn-3.1*, a member of the POU domain transcription factor family, is expressed in sensory hair cells of the inner ear (Erkman et al., 1996; Ryan, 1997; Xiang et al., 1997). In the present study, using *BMP4*, *Fng*, *NT-3*, and *Brn-3.1* as markers, the origin and time at which each sensory organ was molecularly defined in the mouse inner ear were determined.

MATERIALS AND METHODS

Embryos. Pregnant CD-1 mice (Charles River Laboratories, Wilmington, MA) were killed, and the litters were collected according to the *NIH Guide for the Care and Use of Laboratory Animals* protocol. Embryos were individually staged according to the method of Theiler (1989).

Probes. The *in situ* hybridization probe for *Fng* was obtained by

Received Dec. 15, 1997; revised Feb. 18, 1998; accepted Feb. 23, 1998.

This work was supported in part by National Institutes of Health/National Institute on Deafness and Other Communication Disorders Grant DC00139 to A.R. We are indebted to the staff of Biocomputation Center of the Ames Research Center at NASA for their help with ROSS software. We also thank Drs. James Battey and Susan Sullivan for critically reviewing this manuscript, Drs. Brigid Hogan and Linda Erkman for providing plasmids for riboprobe generation, and Mirene Boerner for editing.

Correspondence should be addressed to Dr. Doris K. Wu, National Institute on Deafness and Other Communication Disorders, 5 Research Court, Room 2B34, Rockville, MD 20850.

 0270-6474/98/183327-09$05.00/0

screening an 8.5 d postcoitum (dpc) embryonic mouse λgt10 library (a gift from Brigid Hogan) with a mixture of human (Expressed sequence tags, Research Genetics) and chicken *Fng* (Laufer et al., 1997) cDNAs. Several strongly hybridizing clones were obtained, and one of these, pMFR1, was selected for further analysis. The 2.2 kb insert of pMFR1 contains the entire coding region of murine *Fng* (Cohen et al., 1997; Johnston et al., 1997). The antisense RNA probe was generated by using T3 RNA polymerase after *Hin*dIII restriction digest of pMFR1, and the sense RNA probe was generated by T7 RNA polymerase after *Xba*I restriction digest. The *NT-3* RNA probe was generated from an EST (881879, Genome Systems) containing a fragment of mouse *NT-3* cDNA from the 5′ end of the open reading frame to nucleotide 402 in pT7T3D-Pac vector (Pharmacia, Piscataway, NJ). The *NT-3* antisense RNA probe was generated by using T3 RNA polymerase after restriction digest of the plasmid with *Eco*RI, and the sense RNA probe was generated by using T7 RNA polymerase after restriction digest with *Not*I. The *in situ* hybridization probe for *BMP4* was generated from a 1550 bp full-length mouse *BMP4* cDNA (kindly provided by Brigid Hogan, Vanderbilt University, Nashville, TN) (Jones et al., 1991). For generation of *Brn-3.1* antisense and sense RNA probes, a 209 bp *Xho*I mouse genomic fragment upstream of the POU domain was used (a gift from Linda Erkman, University of California at San Diego, LaJolla, CA). None of the sense RNA probes used in this study yielded any specific hybridization patterns.

Paint injection. Mouse embryos ranging from 10.25 to 17 dpc were harvested and fixed overnight in Bodian's fixative. Specimens were then dehydrated in ethanol and cleared in methyl salicylate. The inner ears were visualized by injecting 0.1% white latex paint in methyl salicylate into the membranous labyrinth as previously described (Martin and Swanson, 1993; Bissonnette and Fekete, 1996). The micropipette was inserted in the lateral surface of otocysts. For more mature ears, the superior ampulla, the utricle, or the common crus were targeted depending on the ease of visualization of the lumen. At a minimum, five inner ears were injected for each stage presented.

Whole-mount in situ *hybridization.* Whole-mount *in situ* hybridization was performed (Riddle et al., 1993) with the following modifications. All embryos were permeabilized with proteinase K (Boehringer Mannheim, Indianapolis, IN) using concentrations from 1 to 15 μg/ml. Hybridization, washings, and detection procedures were performed as described by Riddle et al. (1993).

In situ *hybridization of frozen sections.* Frozen sections of mouse embryos were processed for *in situ* hybridization (Wu and Oh, 1996). Embryos were fixed overnight in 4% paraformaldehyde in PBS, dehydrated in 30% sucrose, and embedded in OCT (Tissue-Tek). Embryos were then sectioned at 12 μm thickness onto superfrost slides (VWR Scientific) and stored at −80°C. Before *in situ* hybridization, slides were warmed to room temperature, rehydrated, post-fixed, and permeabilized using 10 μg/ml proteinase K for 2–5 min. Hybridization was performed in Seal-A-Meal bags (Kapak). Each bag contained four slides and 5 ml of hybridization solution with a probe concentration of ~0.2 μg/ml.

Three-dimensional reconstruction. Images of serial sections of the mouse inner ear after *in situ* hybridization were captured from an Axiophot microscope (Zeiss) onto a Macintosh computer using a CCD camera and NIH Image software. Images were transferred to a Silicon Graphics workstation. Contours of the inner ear of each section were traced, aligned, and reconstructed into three-dimensional images using ROSS software (Biocomputation Center, Ames Research Center, NASA).

RESULTS

Gross anatomy of the developing inner ear

Eight to 12 dpc

The inner ear arose from a thickening of the ectoderm known as the otic placode that invaginated to form an otocyst (data not shown). At 10.75 dpc, a tube-like structure known as the endolymphatic duct projected dorsally from the medial part of the otocyst (Fig. 1*A*, *ed*). In addition, the cochlear anlage emerged as a ventral bulge (Fig. 1*A*, *co*). At 11.5 dpc, the endolymphatic duct was more distinct (Fig. 1*B*, *ed*), and the cochlear anlage continued to expand ventrally (Fig. 1*B*, *co*). The vertical canal plate, which represented the primordium for the posterior and superior semicircular canals, began to form in the dorsolateral part of the otocyst (Fig. 1*B*, *vpl*).

Significant changes occurred at 12 dpc. Two regions in the anterior and posterior parts of the vertical canal plate (Fig. 1*C*, *asterisks*) started to reabsorb, thereby delineating the superior and posterior semicircular canals (Martin and Swanson, 1993). The horizontal canal plate, which is the primordium for the lateral semicircular canal, appeared as a small bulge in the lateral part of the otocyst (Fig. 1*C*, *hp*). The utricle, which houses the macula utriculi, appeared as a protrusion in the anterior part of the inner ear ventral to the vertical plate (Fig. 1*C*, *u*). At this time, the cochlea acquired a more elaborate shape consisting of a proximal and a distal part (Fig. 1*C*, *arrows* and *arrowheads*, respectively). The proximal part extended ventromedially, whereas the distal part started to extend anteriorly, adapting a hook-like shape (Fig. 1*C*, *inset*).

Thirteen to 17 dpc

At 13 dpc, the membranous labyrinth adopted a much thinner and more mature appearance (Fig. 1*D*). The endolymphatic duct became thin, whereas the dorsal portion of the duct formed the primordium for the endolymphatic sac (Fig. 1*D*, *es*). All three canals were well formed (Fig. 1*D*, *ssc*, *psc*, *lsc*), with the superior and posterior semicircular canals joined at the common crus located posterior to the endolymphatic duct (Fig. 1*D*, *cc*). In comparison to the utricle at 12 dpc (Fig. 1*C*, *u*), the floor of the utricle at 13 dpc had adopted a more horizontal orientation (Fig. 1*D*, *u*). The saccular anlage appeared ventral to the utricle as an anterior expansion of the proximal part of the cochlea (Fig. 1*D*, *s*). The proximal part of the cochlea further expanded ventromedially (Fig. 1*D*, *arrows*), whereas the distal part began coiling (Fig. 1*D*, *arrowheads*). The cochlea consisted of half a turn at this point (Fig. 1*D*, *inset*). By 15 dpc, all primordial structures underwent further refinements, approximating their mature shape. The dome-shaped ampullae, which house the cristae, were now apparent (Fig. 1*E*, *sa*, *pa*, *la*). The saccular connections to the utricle and the cochlea, the utriculosaccular and cochleosaccular ducts, respectively, were also apparent at this stage (Fig. 1*E*, *usd*, *csd*). The proximal part of the cochlea expanded further ventromedially (Fig. 1*E*, *arrows*) with its most dorsal tip now being distinct and located anteroventrolateral to the posterior ampulla. The distal part of the cochlea continued to coil (Fig. 1*E*, *arrowheads*) and completed one and one-half turns by 15 dpc (Fig. 1*E*, *inset*). By 17 dpc, the membranous labyrinth had attained its mature shape (Fig. 1*F*), and the coiling process of the cochlea had reached one and three-quarters turns (Fig. 1*F*, *inset*). To demonstrate the relative increase in the size of inner ears from 10.75 to 17 dpc, the structures in Figure 1*A–F* are shown in Figure 1*G* at the same magnification. The *arrows* in Figure 1*G* illustrate the growth of the proximal part of the cochlea from 13 to 17 dpc.

Presumptive sensory organs in the mouse inner ear

In an effort to identify genes that could serve as markers for the presumptive sensory organs in the mouse inner ear, two criteria were imposed: (1) the gene should be activated at an early otocyst stage; and (2) its expression should continue until the sensory organs could be identified histologically. Among multiple genes tested for this purpose, *BMP4* and *Fng* fulfilled both criteria. Results from >30 *in situ* hybridization experiments and three-dimensional reconstructions of critical developmental stages showed that *BMP4* is an early marker for the three cristae in the mouse inner ear, whereas *Fng* is an early marker for the macula

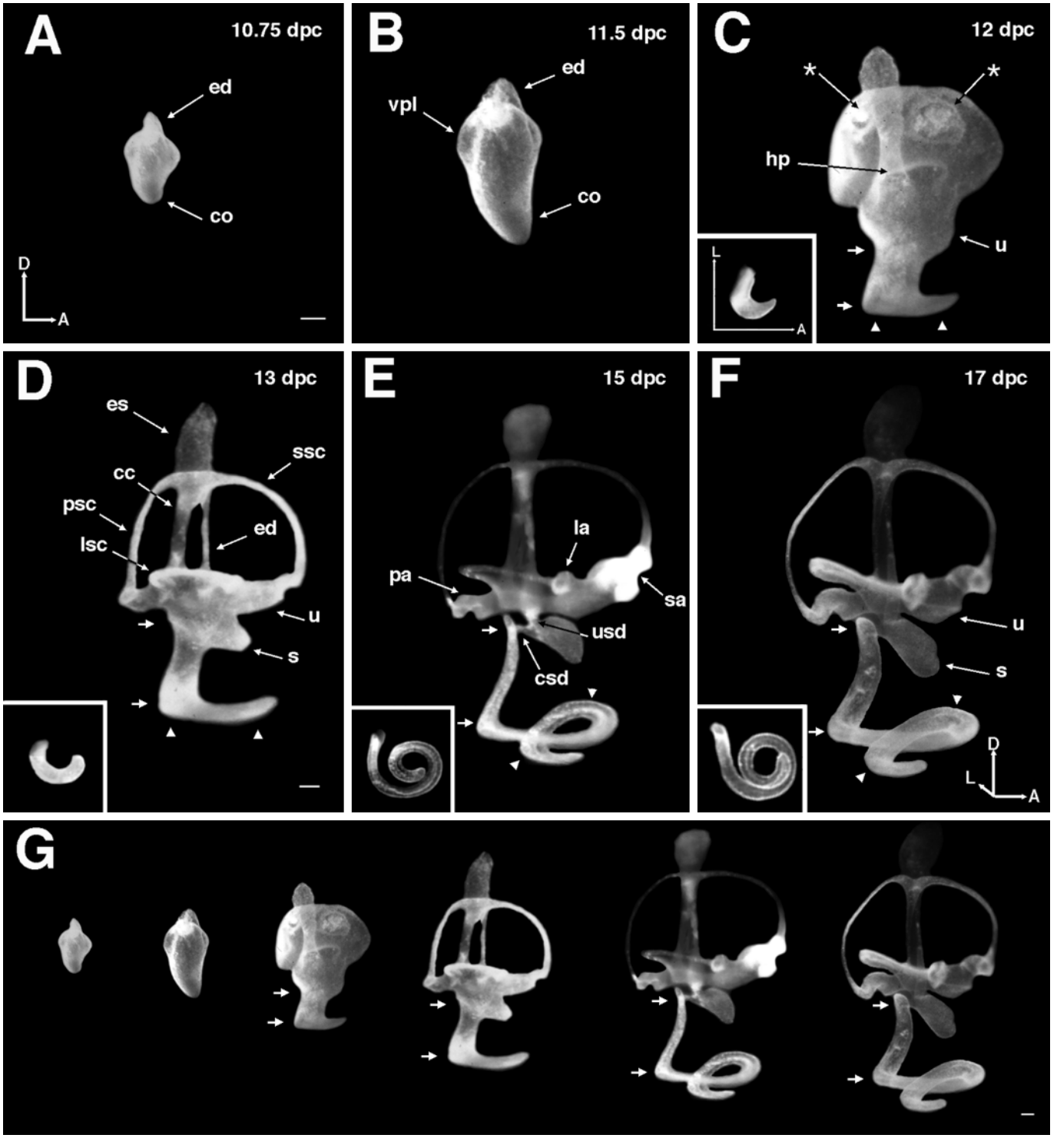

Figure 1. Lateral view of paint-filled membranous labyrinths ranging from 10.75 to 17 dpc. The scale bar and orientation shown in *A* also apply to *B* and *C*. The scale bar and orientation in *D* apply to *E* and *F*. *G* shows all inner ears at the same magnification, with *arrows* illustrating the growth of the proximal part of the cochlea from 13 to 17 dpc. The *insets* at the *bottom left* of *C–F* are ventral views of the cochlea. The orientation shown in *inset* of *C* also applies to *insets* in *D–F*. *Arrows* point to the proximal part of the cochlea; *arrowheads* point to the distal part of the cochlea. *Asterisks* point to areas of reabsorption in the central regions of the developing superior and posterior canals. *cc*, Common crus; *co*, cochlea; *csd*, cochleosaccular duct; *ed*, endolymphatic duct; *es*, endolymphatic sac; *hp*, horizontal canal plate; *la*, lateral ampulla; *lsc*, lateral semicircular canal; *pa*, posterior ampulla; *psc*, posterior semicircular canal; *s*, saccule; *sa*, superior ampulla; *ssc*, superior semicircular canal; *u*, utricle; *usd*, utriculosaccular duct; *vpl*, vertical canal plate. Scale bars, 100 μm.

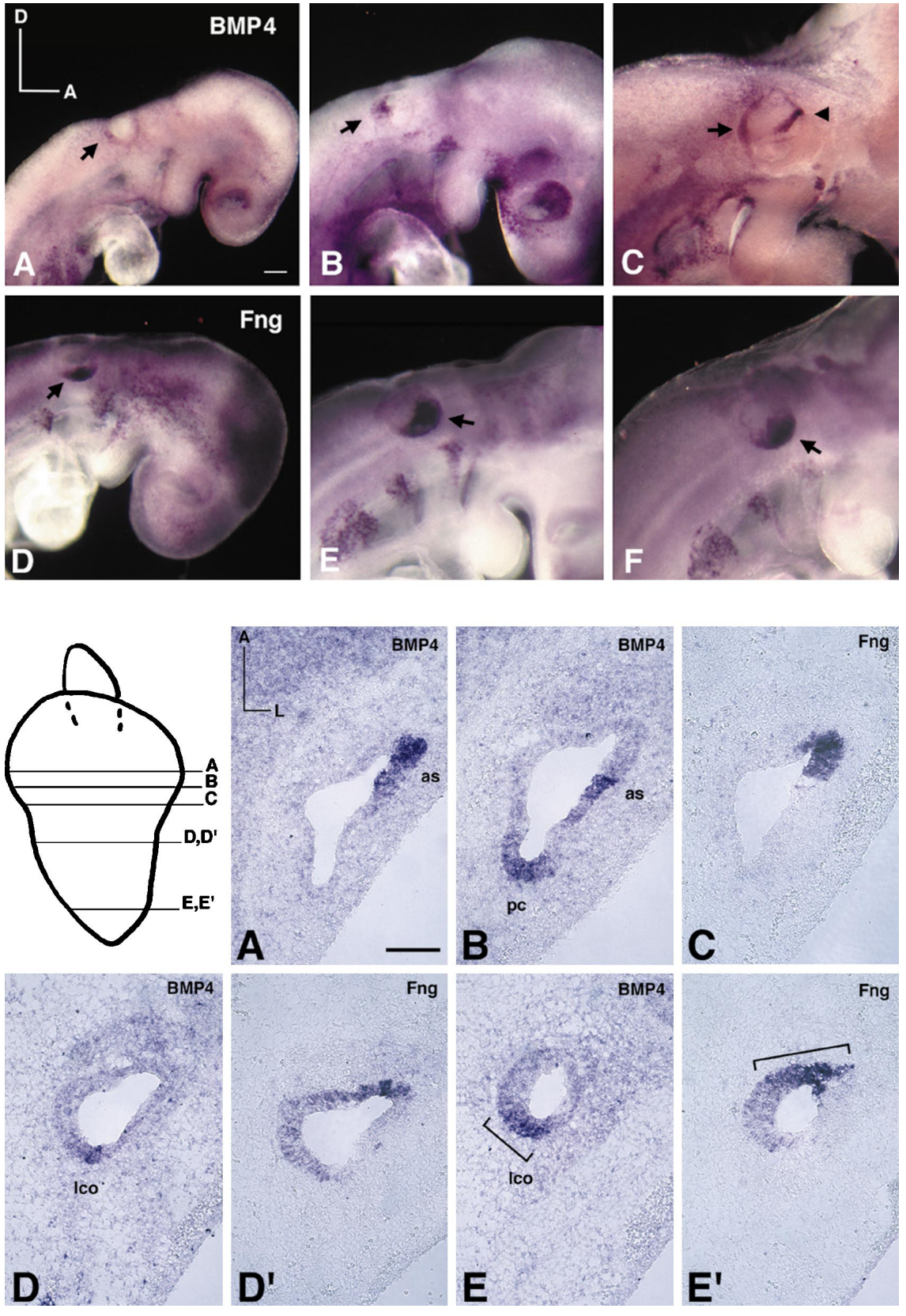

Figure 2. **Top.** Gene expression patterns of *BMP4* and *Fng* in developing mouse inner ear from 9 to 10.25 dpc by whole-mount *in situ* hybridization. At 9 dpc, *BMP4* expression was detected in the posterior margin of the otic cup (*A*, *arrow*), whereas *Fng* transcripts were in the most ventral part of the otic cup (*D*, *arrow*). At 9.5 dpc, *BMP4* was diffusely expressed in the posterior part of the otocyst (*B*, *arrow*). *Fng* transcripts were localized to the most anteroventral part of the otocyst (*E*, *arrow*). At 10.25 dpc, *BMP4* was expressed in two distinct areas, a posterior focus and an anterior streak (*C*, *arrow*, *arrowhead*, respectively). *Fng* transcripts were restricted to the most anteroventral quadrant of the otocyst (*F*, *arrow*). Orientation: *A*, anterior; *D*, dorsal. Scale bar, 100 μm.

utriculi, the macula sacculi, and the cochlea. In both cases, patches of expression initially observed in the otocyst persisted and could be traced until the various sensory structures were well defined both histologically and morphologically. A more detailed account of *BMP4* and *Fng* gene expression during inner ear development is described below.

BMP4 and *Fng* expression from 9 to 11 dpc

Analyses of *BMP4* and *Fng* gene expression patterns during early inner ear development were performed using whole-mount *in situ* hybridization. At 9 dpc when the placode started to invaginate, *BMP4* mRNA was detected in the posterior margin of the otic cup (Fig. 2*A*, *arrow*). At 9.5 dpc, the invagination deepened to form an otocyst. *BMP4* transcripts remained in the posterior portion of the otocyst as a rather diffuse signal (Fig. 2*B*, *arrow*). At 10.25 dpc, the posterior hybridization signal became restricted to a posterior focus (Fig. 2*C*, *arrow*). In addition, a streak of hybridization signal appeared in the anterolateral part of the otocyst (Fig. 2*C*, *arrowhead*). This anterior streak seemed to arise abruptly and independently of the posterior hybridization signal. At 11 dpc, the anterior streak of *BMP4* signal remained the same, whereas the posterior focus expanded ventrally (data not shown).

From 9 to 11 dpc, *Fng* expression was broader than that of *BMP4*. At 9 dpc, *Fng* mRNA was detected in the most ventral portion of the otic cup (Fig. 2*D*, *arrow*). At 9.5 dpc, *Fng* was expressed as a "comma" shape at the most anteroventral part of the otocyst (Fig. 2*E*, *arrow*). By 10.25 dpc, *Fng* expression was restricted to the most anteroventral quadrant of the otocyst (Fig. 2*F*, *arrow*). A similar *Fng* expression pattern was observed at 11 dpc. Although the anterior streak of *BMP4*- and *Fng*-positive areas appeared to be in close proximity to each other at 10.75 and 11 dpc, probing alternate sections for *BMP4* and *Fng* mRNAs indicated that the two positive areas did not overlap with each other (data not shown). Further analyses of *BMP4* and *Fng* expression patterns at later stages were performed using serial cryosections of the inner ear.

BMP4 expression from 11.5 to 13 dpc

At 11.5 dpc, the anterior streak of *BMP4* on the lateral side of the otocyst persisted (Fig. 3*A*,*B*). However, at 12 dpc, this *BMP4* hybridization signal split into an anterior and a lateral focus. These two foci corresponded to the presumptive superior and lateral cristae, respectively (Fig. 4*A*, *sc*, *lc*). The relative positions of the two cristae are illustrated in the three-dimensional reconstruction of a 12 dpc inner ear in Figure 5, *A* and *B*. At 13 dpc, *BMP4* transcripts persisted in the anterior and lateral cristae, as illustrated by the three-dimensional reconstruction of a 13 dpc inner ear (Fig. 5*C*,*D*). By this age, the morphology of the inner ear was more distinct (compare Figs. 1*D*, 5*C*), and the relative positions of the two cristae approximate those of a mature inner ear.

At 11.5 dpc, the posterior focus of *BMP4* signal split into a dorsal spot and a ventral streak, which corresponded to the posterior crista (Fig. 3*B*, *pc*) and the lateral cochlear hybridization signal (lco), respectively (Fig. 3*D*,*E*, *lco*). The lco was located in the posterior pole of the otocyst. It originated ventrolateral to the posterior crista (Fig. 3*D*) and expanded ventrally to the distal tip of the cochlea anlage (Fig. 3*E*). At 12 dpc, *BMP4* transcripts persisted in the posterior crista (Fig. 4*B*, *pc*), whereas the hybridization signal in the lateral cochlea became more complex. The dorsal tip of the lco was restricted and located in the lateral part of the inner ear (Fig. 4*D*, *lco*). As this hybridization signal expanded ventrally, it wrapped around the posterior pole of the inner ear (Fig. 4*E*, *lco*) and continued along the greater curvature of the coiling cochlea (Fig. 4*F*, *lco*). The pattern of the lco can be better appreciated in the three-dimensional reconstruction of the inner ear in Figure 5, *A* and *B*. From this reconstruction, it is apparent that the lco of *BMP4* followed the shape of the future cochlea. This hybridization signal was likened to a ribbon originating anteroventrolateral to the presumptive posterior crista and extending into the greater curvature of the cochlea (compare Figs. 1*E*, 5*A*,*B*). At 13 dpc, *BMP4* transcripts remained in the posterior crista and the greater curvature of the cochlea, as illustrated in the three-dimensional reconstruction in Figure 5, *C* and *D*.

Fng expression from 11.5 to 13 dpc

At 11.5 dpc, the most dorsal boundary of the *Fng*-positive area was ventral to the anterior streak of *BMP4* signal (Fig. 3*C*). This *Fng* signal originated on the anterolateral part of the otocyst and extended both ventrally and medially (Fig. 3*C*,*D*,*E*). In the ventral portion of the otocyst, *Fng* was expressed on the medial side, encompassing the lco of *BMP4* (Fig. 3, compare *D*,*D′*, *E*,*E′*). However, *Fng* transcripts were highly abundant in an anteromedial region (Fig. 3*E*, *brackets*), whereas *BMP4* transcripts concentrated posteromedial to this *Fng*-positive domain (Fig. 3*E*, *brackets*). At 12 dpc, the broad *Fng* expression domain divided into two foci, one dorsal and one ventral. The dorsal focus marked the presumptive macula utriculi, localized in the lateral part of the otocyst, ventral to the presumptive superior and lateral cristae (Figs. 4*C*, 5*A*,*B*, *mu*). The ventral focus was the medial cochlear hybridization signal (mco), localized in the medial part of the otocyst (Fig. 4*E*, *mco*), originating at the level of the cochlear anlage and expanding ventrally into the lesser curvature of the coiling cochlea (Fig. 4*F*, *mco*). *Fng* and *BMP4* transcripts were coexpressed in a small area at the tip of the coiling cochlea (Figs. 4*F*,*F′*, *brackets*, 5*A*, *white stripes*). To determine whether the *BMP4* or *Fng* expression domain gave rise to sensory cells, we compared their expression to other potential presumptive sensory cell markers such as *NT-3* and *Brn-3.1*. *NT-3* proved to be a useful marker in this case. Our results show that the gene expression pattern of *NT-3* was similar to that of *Fng* from 10.75 to 12 dpc (data not shown). The hybridization signal of *NT-3* at 12 dpc overlapped with the *Fng*-positive domain (Fig. 4, compare *F*,*F″*), suggesting that this is the area that will develop into sensory cells.

At 13 dpc, the *Fng* signal in the macula utriculi was more

←

Figure 3. **Bottom.** Gene expression patterns of *BMP4* and *Fng* in developing inner ear at 11.5 dpc. All panels are horizontal sections such that the anterior part of the embryo is toward the *top*. The level of each section is represented in the ear diagram at the *top left*. *D*, *D′*, *E*, and *E′* are 12 μm adjacent sections. *BMP4* was expressed in three distinct areas. In the dorsolateral part of the otocyst, *BMP4* was expressed as an anterior streak (*A*, *B*, *as*). The posterior focus of *BMP4* signal in previous stages had now split into two signals: the posterior crista (*B*, *pc*) and the lateral cochlear hybridization signal (*D*, *E*, *lco*). *Fng* was expressed as one signal originating anterolaterally in the middle of the otocyst (*C*) and expanding ventrally and medially (*D′*, *E′*). At the tip of the cochlea, *Fng* transcripts concentrated in an anteromedial region (*E′*, *brackets*), whereas *BMP4* transcripts concentrated posteromedial to this *Fng* positive domain (*E*, *brackets*). *as*, Anterior streak; *lco*, lateral cochlear hybridization signal; *pc*, posterior crista. Orientation: *A*, anterior; *L*, lateral. Scale bar, 100 μm.

horizontally oriented than at 12 dpc (Fig. 5, compare *A*,*C*). The dorsal part of the mco expanded anteriorly, giving rise to the macula sacculi, as illustrated by the three-dimensional structure (Fig. 5*C*,*D*, *ms*). The ventral part of the mco restricted to the lesser curvature of the cochlea. *Fng* and *BMP4* remained coexpressed in a small area at the tip of the cochlea (Fig. 5*D*, *asterisk*). In addition, at 13 dpc *Fng* transcripts appeared in all three cristae and thus were coexpressed with *BMP4* (Fig. 5*C*,*D*, *sc*, *pc*, *lc*).

BMP4 and *Fng* expression from 14 dpc to postnatal day 1

At 14 and 15 dpc, *BMP4* expression persisted in all three cristae. By 16 dpc, *BMP4* transcripts were concentrated in the supporting cells of the cristae (data not shown). In addition, at 16 dpc *BMP4* was expressed in the supporting cells of the macula utriculi and sacculi (data not shown). From 14 to 18 dpc, the lco of *BMP4* remained localized to the greater curvature of the coiling cochlea.

At 14 dpc, *Fng* expression persisted in all six sensory organs. In addition, the macula sacculi and the cochlea were now distinct based on *Fng* expression pattern. By 16 dpc, *Fng* transcripts concentrated in supporting cells. In the cochlea, the *BMP4*- and *Fng*-positive areas were now juxtaposed. At postnatal day 1 (P1), the histology of the cochlea was more distinct. Figure 6 illustrates *Fng* transcripts being restricted to the supporting cells beneath the differentiating inner and outer hair cells, as indicated by the *Brn-3.1* gene expression pattern (Fig. 6*B*,*C*, *arrows*, *open arrow*, respectively). *BMP4* transcripts were localized to cells lateral to the outer hair cells, which most likely gave rise to Hensen's and/or Claudius' cells (Fig. 6*A*, *arrows*). In addition, at P1 *BMP4* was expressed in the mesenchyme surrounding the cochlea, as previously reported by Takemura et al. (1996) (Fig. 6*A*, *arrowheads*).

DISCUSSION

Morphogenesis of the inner ear

The gross anatomy of the inner ear in several mammalian species has been well described (Retzius, 1884; Larsell et al., 1935; Bast and Anson, 1949). In the mouse, the histology of the inner ear during development has also been described in detail (Kikuchi and Hilding, 1965; Sher, 1971; Lim and Anniko, 1985). However, given the phenomenal morphogenesis that this organ undergoes to reach maturation, it is difficult to correlate the histological differentiation with gross anatomical changes. By using a paint-filling technique previously described (Martin and Swanson, 1993) and three-dimensional reconstructions of gene expression patterns, the development of the sensory organs in relation to the gross anatomy of the inner ear can be appreciated. The ages of the developing inner ears described here were usually 1 d earlier than those previously reported, which is most likely attributable to differences in staging (Theiler, 1989). Nonetheless, the inner ear morphogenesis is in general agreement with previous reports (Sher, 1971; Lim and Anniko, 1985).

Based solely on the paint injection data, one might interpret that the outpouch for the utricle at 12 dpc (Fig. 1*C*, *u*) is actually the primordial structure of the saccule (Fig. 1*D*, *s*). However, three-dimensional reconstructions demonstrating the positions of the sensory organs indicate that this interpretation is incorrect (Fig. 5). The utricle and its macula were located in a vertical position at 12 dpc and became more horizontal by 13 dpc (Figs. 1*C*,*D*, 5*A*,*C*). In contrast, the saccular anlage was not yet apparent at 12 dpc. When the saccule and its macula were distinguishable at 13 dpc, they were located ventral to the utricle and close to the beginning of the first turn of the cochlea (Fig. 5*A*,*B*). As the inner ear matured, the distance between the saccule and the first turn of the cochlea increased considerably (Fig. 1*G*, see distance between *arrows*). Furthermore, study of the paint-injected inner ears showed that the increase in length of the proximal portion of the cochlea occurred concurrently with the coiling of the distal portion.

Origin of sensory organs

BMP4 and *Fng* are expressed early in the otic cup stage and well before the histological differentiation of sensory organs. At these stages, *BMP4* served as a marker for the three cristae, and *Fng* served as a marker for the two maculae and cochlea. Although the expression of these genes overlapped in most sensory organs at older ages, we have used them as markers to determine the time of appearance as well as the approximate location of each presumptive sensory organ in the mouse inner ear. A presumptive sensory organ was considered molecularly defined when either its *BMP4* or *Fng* expression domain was distinct. Based on our results, the posterior crista appeared at 11.5 dpc. The macula utriculi and the superior and lateral cristae appeared at 12 dpc. The macula sacculi and the cochlea were distinguishable at 13 dpc but remained connected until 14 dpc. The location of each presumptive sensory organ described here is consistent with the *in vitro* fate-mapping study of the mouse otocyst performed at 11 and 12 dpc (Li et al., 1978).

An earlier study in chickens using *BMP4* as a sensory organ marker suggested that all sensory organs in the chicken inner ear arise independently from each other (Wu and Oh, 1996). In contrast, results presented here suggest that in the mouse, the superior and lateral cristae may share a common origin as evident by the single *BMP4*-positive area (anterior streak) in the anterior portion of the otocyst that was later seen as two distinct domains. Likewise, the macula utriculi, macula sacculi, and cochlea may share a common origin as well, based on the gene expression patterns of *Fng*. Interestingly, a previous histological study has shown that in some amphibian species, two of the sensory organs (amphibian papilla and papilla neglecta) are initially joined but separated later in development (Fritzsch and Wake, 1988). However, it is important to note that it remains speculative to extrapolate lineage relationships among sensory organs from static images of hybridization signals or histology. Furthermore, because the markers used for sensory organ identification were not identical for the chicken and mouse studies, it is not clear whether these results reflect a fundamental difference in the origin of sensory organ generation between the two species (for model on sensory organ generation in chicken, see Fekete, 1996; Kiernan et al., 1997). Further evidence will have to come from more comparative studies and fate mapping using cell tracers.

Nevertheless, despite the issue of common sensory origin, the shared hybridization areas among the two cristae (superior and lateral) and the two maculae and cochlea suggest that sensory organs may be organized in clusters such that those within a cluster are related to each other developmentally. It has long been suspected that the macula sacculi and the cochlea are developmentally linked. This belief stems from the identification of a group of mutations in mice (Steel and Brown, 1994) and humans (Jackler, 1993) in which only the saccule and the cochlea are affected. In mice, these defects result from a malformation of the stria vascularis, leading to the loss of endocochlear potential within the cochlea (Steel et al., 1987) and subsequent degeneration of sensory hair cells in the sensory organs. Therefore, these defects most likely

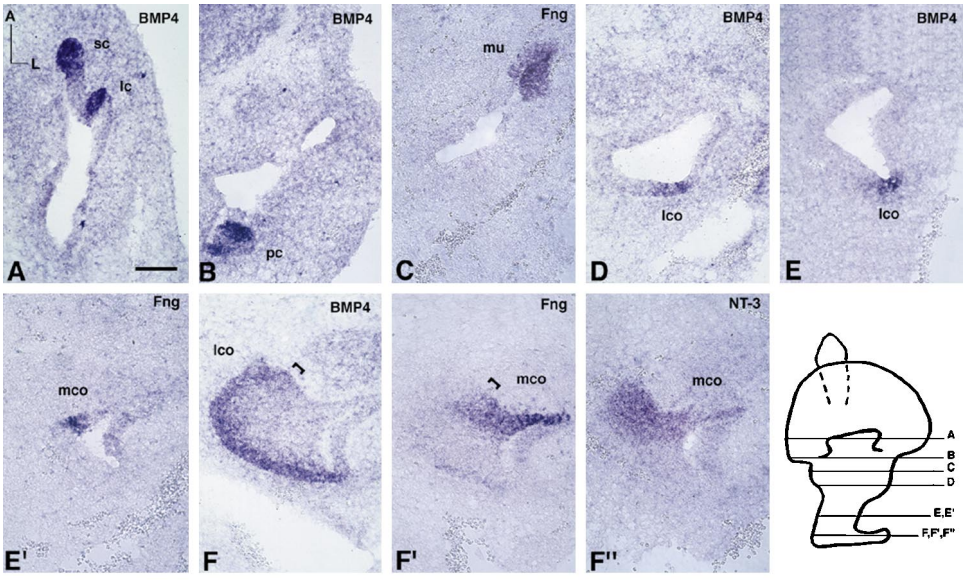

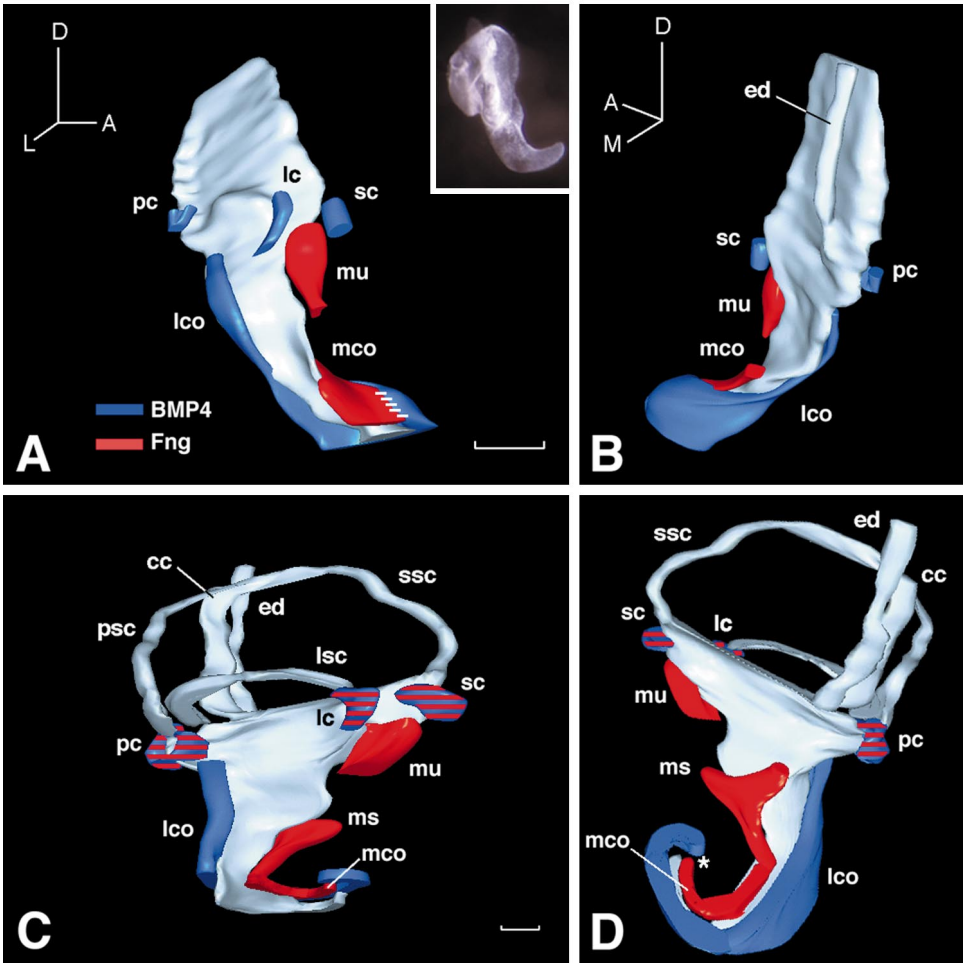

Figure 4. Gene expression patterns of *BMP4* and *Fng* in the developing inner ear at 12 dpc. All panels are horizontal sections such that the anterior part of the embryo is toward the *top*. The level of each section is represented in the ear diagram at the *bottom right*. *F* and *F′* are 12 μm adjacent sections. *BMP4* was expressed in four distinct areas. The anterior streak of *BMP4* signal at 11.5 dpc had now split into the presumptive superior and lateral cristae (*A*, *sc*, *lc*), and *BMP4* was still expressed in the posterior crista (*B*, *pc*). The *lco* of *BMP4* became more elaborate, originating in the lateral part of the inner ear and expanding into the greater curvature of the cochlea (*D*, *E*, *F*, *lco*). *Fng* was expressed in two distinct areas. The most dorsal area was the presumptive macula utriculi (*C*, *mu*). The most ventral area was in the cochlea, where the signal originated in the medial part of the basal turn expanding into the lesser curvature of the cochlea (*E′*, *F′*, *mco*). *BMP4* and *Fng* were coexpressed in a small area at the tip of the cochlea (*F*, *F′*, *brackets*). *NT-3* gene expression overlapped with that of *Fng* in the cochlea (*F″*). *lc*, Lateral crista; *lco*, lateral cochlear hybridization signal; *mco*, medial cochlear hybridization signal; *mu*, macula utriculi; *pc*, posterior crista; *sc*, superior crista. Orientation: *A*, anterior; *L*, lateral. Scale Bar, 100 μm.

Figure 5. Three-dimensional reconstructions of *BMP4* and *Fng* domains of expression in a 12 dpc (*A*, *B*) and 13 dpc (*C*, *D*) mouse inner ear. *BMP4*-positive areas are displayed in *blue*, and *Fng*-positive areas are in *red*. Areas positive for both *BMP4* and *Fng* are in *blue* with *red stripes*. *A* and *C* were tilted to give a ventrolateral view of the right inner ear. *B* and *D* are dorsomedial views. The inner ears of 12 and 13 dpc were reconstructed from 56 and 83 horizontal 12 μm serial sections, respectively. Alternate sections were probed for *BMP4* and *Fng*. The outline of the inner ears was obtained by tracing the inner border of the otic epithelium of each section. The *inset* in *A* is a 12 dpc paint-filled inner ear shown in a view similar to the three-dimensional reconstruction. *White stripes* in *A* represent coexpression of *BMP4* and *Fng* in the distal tip of the cochlea. The *asterisk* in *D* points to the distal tip of the cochlea (not revealed in the reconstruction) where *BMP4* and *Fng* expression overlapped. *cc*, Common crus; *ed*, endolymphatic duct; *lc*, lateral crista; *lco*, lateral cochlear hybridization signal; *lsc*, lateral semicircular canal; *mco*, medial cochlear hybridization signal; *ms*, macula sacculi; *mu*, macula utriculi; *pc*, posterior crista; *psc*, posterior semicircular canal; *sc*, superior crista; *ssc*, superior semicircular canal. Orientation: *A*, anterior; *D*, dorsal; *L*, lateral; *M*, medial. Scale Bars, 100 μm.

reflect the mutual dependence of these two sensory organs for the integrity of the endocochlear potential rather than the fact that they may actually share a common origin. In humans, however, the defects described as cochleosaccular dysplasia are more suggestive of a common developmental problem in the saccule and the cochlea (Ormerod, 1960; Jackler, 1993). The *Fng* expression results described here provide the first molecular evidence that these two sensory organs are developmentally related.

Functions of *BMP4* and *Fng* in inner ear

In most of the sensory organs, both *Fng* and *BMP4* were expressed initially in cells associated with sensory organ formation and later

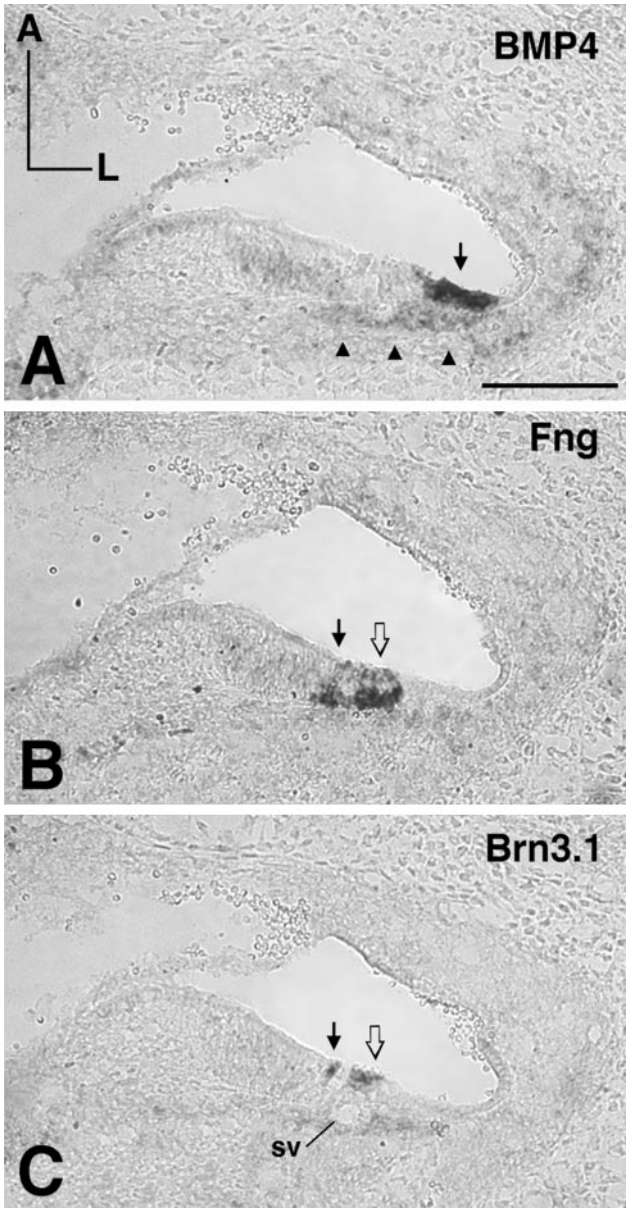

Figure 6. Gene expression of *BMP4*, *Fng*, and *Brn-3.1* in developing cochlea at P1. *A–C* are 12 μm adjacent sections. *BMP4* transcripts were localized to specialized cells lateral to the outer hair cells: Hensen's and/or Claudius' cells (*A*, *arrow*). *BMP4* was also expressed in the mesenchyme surrounding the cochlea (*A*, *arrowheads*). *Fng* transcripts were restricted to the supporting cells underneath the inner and outer hair cells (*B*, *arrow*, *open arrow*, respectively). *Brn-3.1* was expressed in the inner and outer hair cells (*C*, *arrow*, *open arrow*, respectively). *sv*, Spiral vessel. Orientation: *A*, anterior; *L*, lateral. Scale Bar, 100 μm.

in supporting cells. The *Drosophila* fringe protein and its vertebrate homologs, such as lunatic (described in this study), radical, and manic fringe, are thought to specify cell fate through a Notch-signaling pathway (Johnston et al., 1997). Therefore, *Fng* may play an important role in sensory hair cell and supporting cell determination. In addition, fringe proteins are thought to be important in boundary formation during embryogenesis. For example, radical fringe is important for positioning the apical ectodermal ridge at the dorsoventral boundary of the vertebrate limb (Laufer et al., 1997; Rodriguez-Esteban et al., 1997). Lunatic fringe may be important in establishing the boundary of individual somites (Cohen et al., 1997; Johnston et al., 1997). It is interesting that in the mouse cochlea, the *Fng* and *BMP4* domains of expression form a boundary that runs along the third row of outer hair cells, raising the possibility that these genes may play a role in specifying the position of the sensory and nonsensory (i.e., Hensen's and Claudius') cells within the cochlea (Fig. 6).

The early *BMP4* expression pattern in the mouse otocyst is similar to that of the chicken (Wu and Oh, 1996), in which the hybridization signals correspond to the locations of the presumptive cristae. Interestingly, the early *BMP4* expression pattern reported in the *Xenopus* otocyst resembled that of the chicken and mouse, suggesting that *BMP4* is also a marker for the cristae in frogs (Hemmati-Brivanlou and Thomsen, 1995). The conserved pattern of expression across species suggests that *BMP4* may play an important role in the induction and/or differentiation of cristae. In contrast, in the cochlea, expression of *BMP4* is not conserved among chickens and mice. *BMP4* is expressed in the sensory hair cells of the basilar papilla in the chicken (Oh et al., 1996), whereas it is only expressed in Hensen's and/or Claudius' cells of the mouse cochlea. Although the expression domain of *BMP4* was not distributed across the entire lateral wall of the cochlea (Fig. 5*C*), it outlined the shape of the mouse cochlea early in development and was intimately associated with the *Fng*-positive sensory region. Therefore, it would not be surprising if *BMP4* also participates in patterning the shape of the mouse cochlea. In addition, the histology of the mouse cochlea is much more complicated and contains many more cell types than the basilar papilla of the chicken (for review, see Rubel, 1978; Smith, 1985; Cohen and Cotanche, 1992; Fritzsch et al., 1998). The absence of *BMP4* expression in sensory hair cells of the mouse cochlea may contribute to the fine structural differences between the mouse and chicken cochlea. In conclusion, our study serves as a basis for understanding the molecular mechanisms underlying the development of the mammalian inner ear and for deciphering malformations resulting from mutations.

REFERENCES

Bast TH, Anson BJ (1949) The otic labyrinth. In: The temporal bone and the ear, pp 30–105. Springfield, IL: Thomas.

Bissonnette JP, Fekete DM (1996) Standard atlas of the gross anatomy of the developing inner ear of the chicken. J Comp Neurol 174:1–11.

Cohen B, Bashirullah A, Dagnino L, Campbell C, Fisher WW, Leow CC, Whiting E, Ryan D, Zinyk D, Boulianne G, Hui CC, Gallie B, Phillips RA, Lipshitz HD, Egan SE (1997) Fringe boundaries coincide with Notch-dependent patterning centres in mammals and alter Notch-dependent development in *Drosophila*. Nat Genet 16:283–288.

Cohen GM, Cotanche DA (1992) Development of the sensory receptors and their innervation in the chick cochlea. In: Development of auditory and vestibular systems, Vol 2 (Romand AL, ed), pp 101–138. New York: Elsevier.

Erkman L, McEvilly RJ, Luo L, Ryan AK, Hooshmand F, O'Connell SM, Keithley EM, Rapaport DH, Ryan AF, Rosenfeld MG (1996) Role of transcription factors Brn-3.1 and Brn-3.2 in auditory and visual system development. Nature 381:603–606.

Fekete DM (1996) Cell fate specification in the inner ear. Curr Opin Neurobiol 6:533–541.

Fritzsch B, Wake MH (1988) The inner ear of gymnophione amphibians and its nerve supply: a comparative study of regressive events in a complex sensory system (*Amphibia*, *Gymnophiona*). Zoomorphology 108:201–217.

Fritzsch B, Farinas I, Reichardt LF (1997a) Lack of neurotrophin-3 causes losses of both classes of spiral ganglion neurons in the cochlea in a region-specific fashion. J Neurosci 17:6213–6225.

Fritzsch B, Farinas I, Reichardt L (1997b) The development of NT-3 expression as revealed with a Lac-Z reporter and of innervation deficits in NT-3 mutant mice. Soc Neurosci Abstr 23:351.13.

Fritzsch B, Barald K, Lomax M (1998) Early embryology of the verte-

brate ear. In: Development of the auditory system, Springer handbook of auditory research (Rubel E, Popper A, Fay RS, eds), pp 81–145. New York: Springer.
Hemmati-Brivanlou A, Thomsen GH (1995) Ventral mesodermal patterning in *Xenopus* embryos: expression patterns and activities of BMP-2 and BMP-4. Dev Genet 17:78–89.
Jackler RK (1993) Congenital malformations of the inner ear. In: Otolaryngology–head and neck surgery, Vol 4 (Patterson AS, Ryan JD, eds), pp 2756–2771. St. Louis: Mosby.
Johnston SH, Rauskolb C, Wilson R, Prabhakaran B, Irvine KD, Vogt TF (1997) A family of mammalian fringe genes implicated in boundary determination and the Notch pathway. Development 124:2245–2254.
Jones MC, Lyons KM, Hogan BLM (1991) Involvement of bone morphogenetic protein-4 (BMP-4) and Vgr-1 in morphogenesis and neurogenesis in the mouse. Development 111:531–542.
Kiernan AE, Nunes F, Wu DK, Fekete DM (1997) The expression domain of two related homeobox genes defines a compartment in the chicken inner ear that may be involved in semicircular canal formation. Dev Biol 191:215–229.
Kikuchi K, Hilding D (1965) The development of the organ of Corti in the mouse. Acta Otolaryngol 60:207–222.
Larsell O, McCrady E, Zimmermann A (1935) Morphological and functional development of the membranous labyrinth in the opossum. J Comp Neurol 63:95–118.
Laufer E, Dahn R, Orozco OE, Yeo CY, Pisenti J, Henrique D, Abbott UK, Fallon JF, Tabin C (1997) Expression of radical fringe in limb-bud ectoderm regulates apical ectodermal ridge formation. Nature 386:366–373.
Li CW, Van Der Water TR, Ruben RJ (1978) The fate mapping of the eleventh and twelfth day mouse otocyst: an *in vitro* study of the sites of origin of the embryonic inner ear sensory structures. J Morphol 157:249–268.
Lim DJ, Anniko M (1985) Developmental morphology of the mouse inner ear. Acta Otolaryngol Suppl 422:1–69.
Martin P, Swanson GJ (1993) Descriptive and experimental analysis of the epithelial remodellings that control semicircular canal formation in the developing mouse inner ear. Dev Biol 159:549–558.
Oh SH, Johnson R, Wu DK (1996) Differential expression of bone morphogenetic proteins in the developing vestibular and auditory sensory organs. J Neurosci 16:6463–6475.
Ormerod FC (1960) The pathology of congenital deafness. J Laryngol Otol 74:919–950.
Retzius G (1884) Das Gehörorgan der Wirbeltiere: II Das Gehörorgan der Amnioten, pp 201–358. Stockholm: Samson und Wallin.
Riddle RD, Johnson RL, Laufer E, Tabin C (1993) Sonic hedgehog mediates the polarizing activity of the ZPA. Cell 75:1401–1416.
Rodriguez-Esteban C, Schwabe JWR, De La Pena J, Foys B, Eshelman B, Belmonte JCI (1997) Radical fringe positions the apical ectodermal ridge at the dorsoventral boundary of the vertebrate limb. Nature 386:360–366.
Rubel EW (1978) Ontogeny of structure and function in the vertebrate auditory system. In: Handbook of sensory physiology: development of sensory systems, Vol 9 (Jacobson M, ed), pp 135–237. New York: Springer.
Ryan AF (1997) Transcription factors and the control of inner ear development. Semin Cell Dev Biol 8:249–256.
Sher A (1971) The embryonic and postnatal development of the inner ear of the mouse. Acta Otolaryngol Suppl 285:1–77.
Smith CA (1985) Inner ear. In: Form and function in birds, Vol 3, (King AS, McLelland J, eds) pp 273–310. London: Academic.
Steel KP, Barkway C, Bock G (1987) Strial dysfunction in mice with cochleo-saccular abnormalities. Hear Res 27:11–26.
Steel KP, Brown SDM (1994) Genes and deafness. Trends Genet 10:428–435.
Takemura T, Sakagami M, Takebayashi K, Masanori U, Nakase T, Takaoka K, Kubo T, Kitamura Y, Nomura S (1996) Localization of bone morphogenetic protein-4 messenger RNA in developing mouse cochlea. Hear Res 95:26–32.
Theiler K (1989) The house mouse: atlas of embryonic development. New York: Springer.
Wheeler EF, Bothwell M, Schecterson LC, von Bartheld CS (1994) Expression of BDNF and NT-3 mRNA in hair cells of the organ of Corti: quantitative analysis in developing rats. Hear Res 73:46–56.
Wu DK, Oh SH (1996) Sensory organ generation in the chick inner ear. J Neurosci 16:6454–6462.
Xiang M, Gan L, Li D, Chen ZY, Zhou L, O'Malley BWJ, Klein W, Nathans J (1997) Essential role of POU-domain factor Brn-3c in auditory and vestibular hair cell development. Proc Natl Acad Sci USA 94:9445–9450.
Ylikoski J, Pirvola U, Moshnyakov M, Palgi J, Arumae U, Saarma M (1993) Expression patterns of neurotrophin and their receptor mRNAs in the rat inner inner ear. Hear Res 65:69–78.